Energy Consumption of the Mobile Wireless Sensor Network's Node with Controlled Mobility

Konstantin Mikhaylov and Jouni Tervonen
RFMedia Laboratory
Oulu Southern Institute, University of Oulu
Ylivieska, Finland
{konstantin.mikhaylov, jouni.tervonen}@oulu.fi

Abstract— **One of the recent tendencies for Wireless Sensor Networks (WSNs) that significantly increases their performance and functionality is the utilization of mobile nodes. The paper discusses in detail the structure of a WSN node with controlled mobility and presents the energy consumption measurement results for the real-life mobile WSN node platform in different operation modes. As the presented results reveal, besides the actual energy consumption by the radio during communication or by the motors during movement, one must also account the consumption by the voltage conversion and stabilization circuits and by the sensors.**

Keywords-wireless sensor networks; energy; consumption; mobility; WSN; platform; node; test; measurement; evaluation

I. INTRODUCTION

The contemporary Wireless Sensor Networks (WSNs) have a very broad application area and are becoming the important part of everyday life. One of the recent tendencies for WSNs is the extension of their functionality and performance by means of using mobile WSN nodes.

The node mobility in a WSN can be classified using three major terms: the mobility subject (i.e., what is the role of mobile nodes), the nature of mobility (i.e., what is the mobility purpose) and the available data about mobility and node locations [1].

As has been shown in the recent studies, a mobile WSN node can be used to increase the WSN coverage or precision, the reliability, energy efficiency or other quality of service (QoS) parameters for the communication [2]–[7]. However, the presence of a mobile node in a WSN introduces multiple novel challenges: e.g., the requirement for localization techniques and mechanisms for detecting the contact between mobile and static nodes; the dynamic network topology change depending on mobile node position; the power and resource management for mobile and static nodes [2], [3].

The problem of energy efficiency and power management is very important for WSNs due to restricted resource availability for the majority of these systems [3], [8]. However, for WSN with mobile nodes this problem gets additional value as, unlike the static nodes that can use mains to get the energy for their operation, the mobile ones usually have to use the energy stored in the primary or secondary batteries. Furthermore, for the controlled mobility scenario, the energy for moving the node mostly often also comes from its batteries.

Unfortunately, up to now there have been introduced and implemented in hardware only a few mobile WSN (MWSN) nodes and only some scattered pieces of information concerning their energy consumption were presented in the existing research works. E.g., in [9] for testing the suggested network infrastructure authors have used the prototype of a mobile node based on PackBot [10] and reported that its energy consumption during movement was *60J/m*. In [11] has been reported the measurements for the mobility of PackBot 4a and Rhex-R platforms and presented their energy consumption for moving on-road (*59 m/Wh* and *27 m/Wh* respectively) and off-road (*40m/Wh* and *22 m/Wh* respectively). In [12], [13] the authors have investigated the operation of the motors, estimated the energy consumption for WSN node movement and obtained the value of *2 J/m* for the optimal motor operation mode. The same value (although without providing any clarification) has been used in [14]. Nonetheless, in the majority of the current research works considering the WSN nodes mobility, the energy consumption of the nodes for mobility is not taken into account at all (consider e.g., [15]–[18]).

Therefore, in the current paper, we focus specifically on the problem of energy consumption for the real MWSN node platform using as the reference the EVALBOT [19] platform from Texas Instruments. In the paper we define the modules that affect the energy consumption of a WSN node and in detail investigate the influence of various parameters on mobile node energy consumption.

II. ARCHITECHTURE OF A MOBILE WSN NODE

The typical architecture of a WSN node with controlled mobility is presented in Fig. 1. As revealed in Fig. 1 the node usually consists of five major components.

The first one is the *source of power* that provides the energy for the whole system and that is usually represented by the primary or secondary batteries. Often, the other components of the MWSN node are receiving the power not from the power source directly, but through the *special voltage conversion* and *regulation circuitry*. Those circuits are used to up- or down-convert and stabilize the voltage to the levels required for each particular component. Depending on the used peripherals, the MWSN node can require to have multiple intermediate voltages. Naturally,

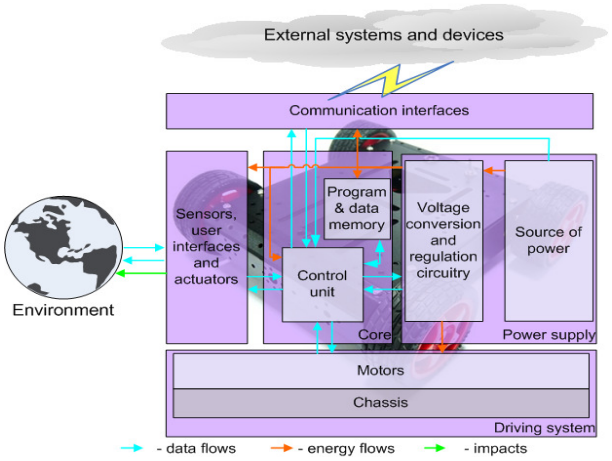

Figure 1. Typical architecture of a MWSN node with controlled mobility.

even if the peripheral connected to these voltage lines is not currently used and stay in low-power mode, the voltage conversion circuits themselves consume some energy (consider, e.g. [20]).

The second component is the *control unit* that controls the operation of the mobile WSN node and the required peripherals, such as the read-only memory (ROM) for program storage and random access memory (RAM) for temporal data storage. In case if the WSN node is controlled by a microcontroller, the external memory chips are usually not required [20].

The third component of the MWSN node is the set of all *sensors*, *actuators* and *user interfaces*. Besides the actual sensors required by the application, the MWSN node usually needs some additional ones for enabling its mobility. In the most general case, those include the sensors required for MWSN node localization and obstacle/collision detection, navigation and movement control (e.g., speed measurement).

The fourth component of the MWSN node is the *chassis* and the *motors* to enable node movement. Depending on the application, the MWSN node can require to move over air, water or ground and the used chassis can differ significantly. In the current paper, we will focus on the scenario of movement over the ground as it is the most common today. For the movement over the ground, three major options for the chassis can be used: the wheels, the caterpillars and the walking legs [13]. As reported in [13], the wheels are often used for MWSN application due to their low cost and easy manipulation. To transform the electrical energy into the mechanical energy required for wheel or caterpillar rotation or leg movement the MWSN nodes use the motors. For enabling the movement direction change, the node usually requires to have at least two motors (for wheel or caterpillar chassis).

The final component of the MWSN node is the set of *communication interfaces* (i.e., the set of wireless and/or wired transceivers). Depending on the application and

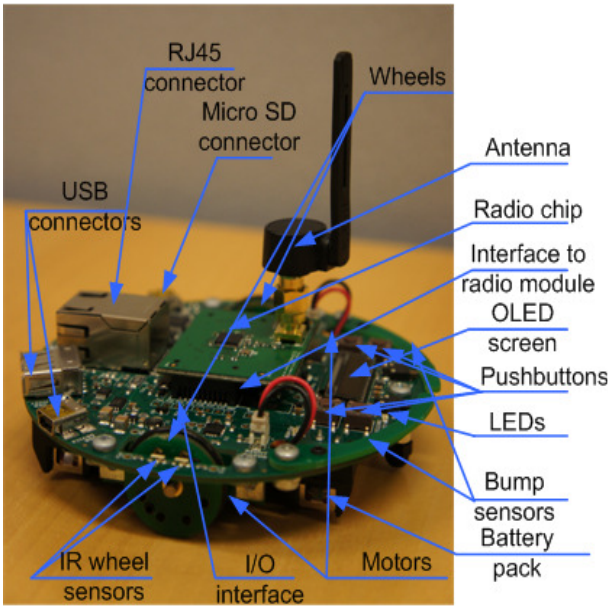

Figure 2. TI EVALBOT with installed CC2430 radio module.

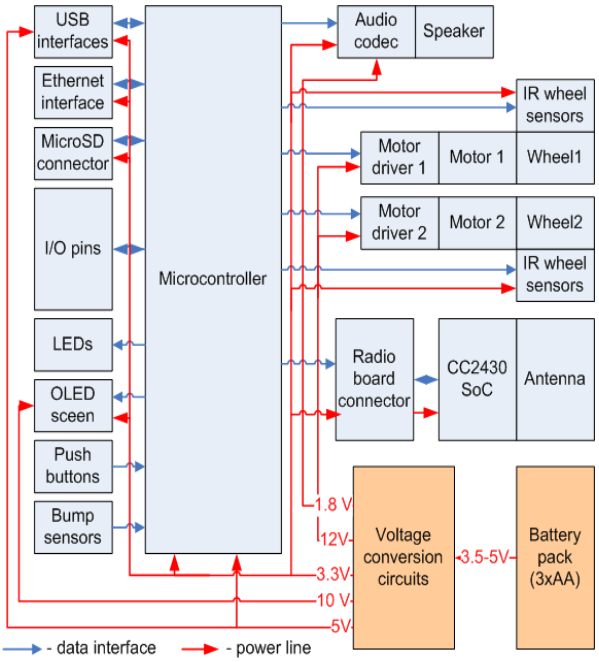

Figure 3. Block structure of TI EVALBOT + CC2430 MWSN node used in the tests.

environment, the MWSN can use ultrasonic [21], optical [22], [23], or radio communication. For the ground scenario, the radio communication is usually chosen.

III. TESTBED MOBILE WSN PLATFORM DESCRIPTION

For our tests we have used the EVALBOT [19] platform from Texas Instruments (TI) presented in Figs. 2 and 3. The EVALBOT is implemented as the circular printed circuit board with 10cm diameter and with the installed 2.4 GHz radio board has the height around 9.5 cm (up to the top of the swivel antenna). The total weight of the platform with

TABLE I. CURRENT CONSUMPTION OF MOBILE WSN NODE PERIPHERALS

Supply voltage, V	Controller clock, MHz	LED1	LED2	OLED display	Motor left, rpm	Motor right, rpm	Wheel sensor left	Wheel sensor right	Radio	Current consumption, mA
5	-[a]	UI[b]	UI[b]	UI[b]	UI[b]	UI[b]	UI[b]	UI[b]	UI[b]	76.7
5	sleep	UI[b]	UI[b]	UI[b]	UI[b]	UI[b]	UI[b]	UI[b]	UI[b]	85.5
5	4	UI[b]	UI[b]	UI[b]	UI[b]	UI[b]	UI[b]	UI[b]	UI[b]	86.3
5	10	UI[b]	UI[b]	UI[b]	UI[b]	UI[b]	UI[b]	UI[b]	UI[b]	89.9
5	16	UI[b]	UI[b]	UI[b]	UI[b]	UI[b]	UI[b]	UI[b]	UI[b]	92
5	20	UI[b]	UI[b]	UI[b]	UI[b]	UI[b]	UI[b]	UI[b]	UI[b]	95.4
5	50	UI[b]	UI[b]	UI[b]	UI[b]	UI[b]	UI[b]	UI[b]	UI[b]	110
5	16	ON	UI[b]	UI[b]	UI[b]	UI[b]	UI[b]	UI[b]	UI[b]	95
5	16	ON	ON	UI[b]	UI[b]	UI[b]	UI[b]	UI[b]	UI[b]	98.1
5	16	UI[b]	UI[b]	Black	UI[b]	UI[b]	UI[b]	UI[b]	UI[b]	114
5	16	UI[b]	UI[b]	Half-white	UI[b]	UI[b]	UI[b]	UI[b]	UI[b]	120
5	16	UI[b]	UI[b]	White	UI[b]	UI[b]	UI[b]	UI[b]	UI[b]	126
5	16	UI[b]	UI[b]	UI[b]	0	UI[b]	UI[b]	UI[b]	UI[b]	113
5	16	UI[b]	UI[b]	UI[b]	10	UI[b]	UI[b]	UI[b]	UI[b]	118
5	16	UI[b]	UI[b]	UI[b]	50	UI[b]	UI[b]	UI[b]	UI[b]	134
5	16	UI[b]	UI[b]	UI[b]	99	UI[b]	UI[b]	UI[b]	UI[b]	153
5	16	UI[b]	UI[b]	UI[b]	UI[b]	-99[3]	UI[b]	UI[b]	UI[b]	153
5	16	UI[b]	UI[b]	UI[b]	99	99	UI[b]	UI[b]	UI[b]	192
5	16	UI[b]	UI[b]	UI[b]	UI[b]	UI[b]	on	on	UI[b]	156
5	16	UI[b]	UI[b]	UI[b]	UI[b]	UI[b]	UI[b]	UI[b]	RX[4]	113.5
5	16	UI[b]	UI[b]	UI[b]	UI[b]	UI[b]	UI[b]	UI[b]	RX[5]	111.5
5	16	UI[b]	UI[b]	UI[b]	UI[b]	UI[b]	UI[b]	UI[b]	TX: 0.6dBm	116.7
5	16	UI[b]	UI[b]	UI[b]	UI[b]	UI[b]	UI[b]	UI[b]	TX: -0.4dBm	111.2
5	16	UI[b]	UI[b]	UI[b]	UI[b]	UI[b]	UI[b]	UI[b]	TX: -5.7dBm	105.5
5	16	UI[b]	UI[b]	UI[b]	UI[b]	UI[b]	UI[b]	UI[b]	TX: -25.2dBm	102

a. microcontroller and all peripherals are in reset mode
b. uninitialized
c. reverse rotation direction
d. no radio signal
e. strong radio signal (RSSI: -40 dBm)

installed radio module and three AA alkaline batteries is 189 g (without batteries – 118 g). The node is controlled by the LM3S9B92 32-bit ARM® Cortex™ with the processor core that supports clock frequency up to 80 MHz [24]. The microcontroller has 256 kB single-cycle Flash and 96 kB single-cycle Static RAM [24] on-chip. For the movement, the EVALBOT is equipped with two 12V motors that are controlled by the microcontroller through motor driver circuits. The motors rotate two 2.4 cm diameter wheels. The actual speed of the wheel rotation can be measured using 2 infra-red (IR) sensors installed near each wheel. Besides the motors, the EVALBOT contains: several light-emitting diodes (LEDs) and pushbuttons, 96x6 organic LED (OLED) display, audio codec and speaker, MicroSD card connector, RJ45 Ethernet connector and USB connectors. Also, the board has several lines connected to microcontroller General Purpose Input/Output (GPIO) pins that can be used for connecting external peripherals and the connector for connecting wireless boards from TI. For our tests, we have attached to EVALBOT the CC2431 IEEE 802.15.4-compatible radio boards from TI [25].

As revealed in Fig. 3, to meet the on-node peripherals requirements, the voltage conversion circuits convert the voltage obtained from the batteries into five different constant voltages, namely: 1.8V; 3.3V; 5V; 10V and 12V.

IV. MEASUREMENT METHODOLOGY AND RESULTS

To measure the current consumption for mobile WSN node components we have used the test-bed presented in Fig. 4. The embedded software that has been developed for

TABLE II. EFFECT OF SUPPLY VOLTAGE ON THE CURRENT CONSUMPTION OF MOBILE WSN NODE WITH ACTIVE RADIO (both radio and SoC microcontroller core are active)

Radio mode	Value in transmit power register	Radio transmit power, dBm(mW)	Current consumption, mA		
			Vbat 4V	Vbat 4.5V	Vbat 5.5V
TX[a]	3	-25.9	100.9	100.4	102.0
TX[a]	5	-19.7	102.3	100.6	102.3
TX[a]	7	-16.4	102.7	101.1	102.8
TX[a]	9	-13.2	103.0	101.8	103.3
TX[a]	11	-11.0	103.9	102.2	103.9
TX[a]	15	-8.1	104.8	103.8	105.0
TX[a]	19	-6.1	105.4	104.6	105.5
TX[a]	27	-2.9	107.5	106.4	107.8
TX[a]	95	-0.8	110.2	110.2	111.2
TX[a]	255	0.6	115.9	115.8	116.7
RX[b]	-	-	112.7	112.3	113.5
RX_PKT[c]	-	-	112.6	111.3	111.5

a. – radio transmit
b. – radio receive (no signal)
c. – radio receive (strong signal)

the MWSN node testing allowed to control each peripheral device separately. The measurements for energy consumption, as revealed in Fig. 4, were done using the current-shunt method that is well proven for energy consumption measurements for embedded systems and WSN nodes [26]–[28]. The results revealing the current consumption of the MWSN node peripherals are revealed in Table I and Fig. 5. The maximum instrumentation error for these results is below 1 mA. The first thing that can be noticed from the presented data in Table I is that the MWSN

node had very high current consumption in reset mode when no system on the node was actually functioning. We assume that the majority of this consumption is caused by the voltage conversion and stabilization circuits.

As revealed in Table I, to minimize the energy consumption per computed instruction the microcontroller on MWSAN node should run at high clock frequencies (compare with [20]). The utilization of user interfaces on MWSN, as can be seen from the presented data, increased the consumption of the MWSN node by approximately 3mA for each LED and by 19 to 31 mA for 96x6 OLED display. For the latter one, the consumption depends on the number of the segments that are used. The consumption by the motors for the tested scenario (the measurements were done with the robot running on a flat wooden surface) depends on the wheels rotation speed almost linearly and was the same for both motors and both directions. Also, as can be seen from the presented data, the IR sensors, which measured the actual wheel rotation speed and the passed way, consume almost as much energy as both motors running with 60 revolutions per minute. The active radio module increased the current consumption of the node by around 21 mA for radio in the receive mode and by 10-25 mA for radio transmission depending on used transmission power (see Fig.6).

As can be seen from Fig. 5, although the MWSN node is equipped with voltage regulation circuits, its current consumption was changing depending on the supply voltage. Besides, the trends to supply voltage effect on the current consumption differ for various components. So, the current consumed by the MWSN node components that required voltage up-conversion (i.e., OLED display and motors – see Fig. 3) decreased with the increase of the voltage while for the other peripherals increase of supply voltage increased the current consumption as well. As the current consumption for the display and motors are affected by the supply voltage change more significantly, the total energy consumption for the MWSN with all peripherals active decreased with the increase of the supply voltage (see Fig.5).

As revealed in Table II the current consumption by the CC2431 radio module used on MWSN is defined by the working mode of the radio. With the radio in receive mode, the current consumption of the MWSN node increased by around 19-21 mA. Note, that the consumption by the radio for the cases when there was no radio signal and when the radio transmission was going on is slightly different. This is caused by the Automatic Gain Control (AGC) system in the radio. As can be seen in Fig. 6, the dependence of the current consumed by the radio from the radiated radio signal power is quite close to linear. Nonetheless, as revealed in Fig. 6 and Table II, even with the minimum transmit power sittings the radio consumes at least 10 mA. As reveal Table II, the battery voltage level (Vbat) of the MWSN node was not significantly influencing the consumed by the radio current. Fig. 7 illustrates the typical operations sequence for

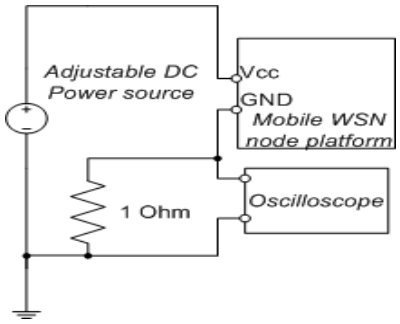

Figure 4. Experiment set-up used for measuring the consumption of the mobile WSN node.

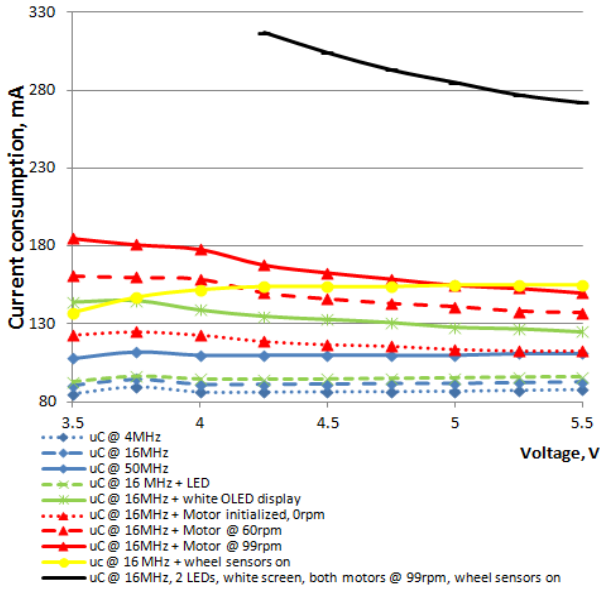

Figure 5. Effect of supply voltage on current consumption of the MWSN platform.

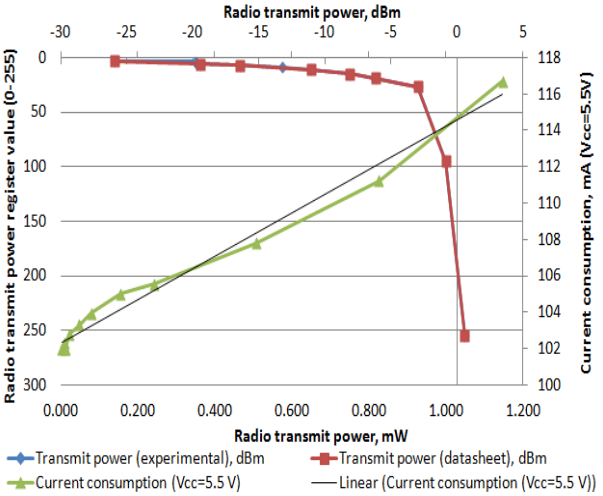

Figure 6. Effect of radio module's transmission power setting on radiated radio signal power

radio packet transmission, the lengths and the current consumption at different stages. As can be seen, to send the

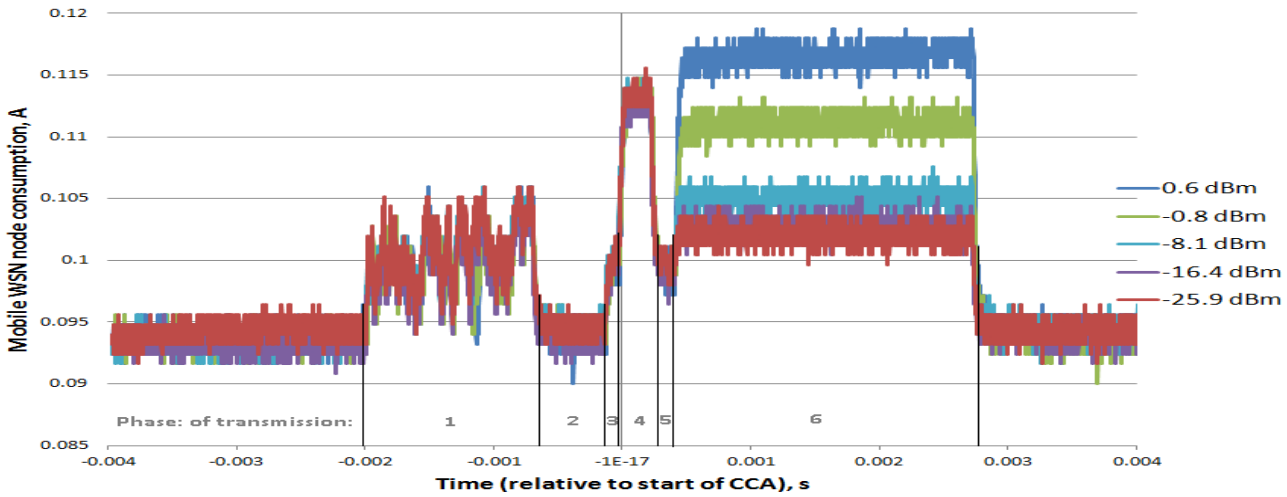

Figure 7. Effect of radio module transmission power (see Fig. 6) on the current consumption of MWSN node at 5.5V power supply (packet payload 55 bytes)

data via radio the MWSN node controller first of all transmits the data to the radio (phase **1**) using the wired interface (in tested case radio and microcontroller of MWSN node were connected over UART [28] interface with 115200 bit/s data rate). After that, the microcontroller core of CC2430 processes the received data (phase **2**) and activates the radio. After radio start-up and calibration (phase **3**), it switches to the receive mode to check the radio channel (phase **4**). Finding that the channel is free, the radio recalibrates itself (phase **5**) and finally sends the data (phase **6**). Once the packet is transmitted, the radio is switched off.

V. Discussion and Conclusions

The results presented in the paper reveal that the consumption of the tested platform motors was around 2-3 J per meter of the way depending on the supply voltage level. This is quite close to the analytic results obtained and used e.g., in [12-14]. Nonetheless, the results of the measurements for real hardware reveal that besides the actual energy consumption by the motors on MWSN node, one should also consider the consumption by the other components. For the tested platform, the current consumption by the voltage conversion and stabilization circuits was in the order of 70-80 mA, which is as much as the consumption by the motors running at half speed. Besides, the tested platform, as well as many other contemporary mobile platforms, has *no means to control or disable the voltage conversion circuits*. This is allowable in the case if the MWSN node moves all the time, but if the mobility of the MWSN node is sporadic (which is assumed for many suggested MWSN applications and protocols – e.g., [29], [30]) this will significantly reduce the lifetime of the mobile node. The presented in the paper results reveal that with active radio and inactive motors, around 66% of the total energy consumed by the MWSN node is used by the voltage conversion circuitry. Besides, to control the movement the MWSN node requires extra sensors for measuring the speed of node movement and passed distance. As revealed in the paper, the consumption for those is also quite significant and is comparable to the consumption of the motors. The consumption of the radio module depends on the working mode of the radio. For the tested module it ranged from 10 to 25 mA during radio packet transmission and was around 21 mA during radio reception.

The current paper is the first, to the best of our knowledge, which focuses and in detail discusses the structure and the energy consumption of the miniature mobile WSN node platform with controlled mobility. We are sure that the data presented in the paper are valuable both for the WSN practitioners and for researchers. For the former ones, the data presented in the paper provides valuable information for MWSN nodes hardware design, possibilities and features for such nodes. For the latter ones, the presented data allows a better understanding about the behavior of the MWSN nodes and allows improving the MWSN simulation accuracy.

Although the presented in the paper measurements have been executed only for the single MWSN node platform, we are sure that the revealed in the paper general dependences will be similar also for the other platforms. In the future we will consider extending the measurements presented in the paper by also testing other MWSN platforms to prove this. Besides, we will continue the work with the described MWSN platform and test its behavior in real-life MWSN applications.

Acknowledgment

The authors wish to thank all parties who have financially supported this study. This work has been supported by European Regional Development Fund, Council of Oulu Region, Ylivieska Subregion, Ylivieska Town, Kerttu Saalasti Foundation, and NIHAK development organization.

The authors also wish to thank the reviewers for valuable contributions and comments on the earlier version of this article.

REFERENCES

[1] K. Mikhaylov and J. Tervonen, "Data collection from isolated clusters in wireless sensor networks using mobile ferries," Proc. The International Symposium on Frontiers of Information Systems and Network Applications (FINA'13(WAINA'13)), in press, Mar. 2013.

[2] M. Di Francesco, S. K. Das, and G. Anastasi, "Data collection in wireless sensor networks with mobile elements: a survey," ACM Trans. Sen. Netw., vol. 8, no. 1, Aug. 2011, pp. 7:1–7:31, doi:10.1145/1993042.1993049.

[3] J. Rezazadeh, M. Moradi, and A. S. Ismail, "Mobile Wireless Sensor Networks Overview," Int. J. of Computer Communications and Networks, vol. 2, no. 1, Feb. 2012, pp. 17 –22.

[4] M. Marta and M. Cardei, "Using sink mobility to increase wireless sensor networks lifetime," Proc. International Symposium on a World of Wireless, Mobile and Multimedia Networks (WOWMOM'08), IEEE Press, Jun. 2008, pp. 1–10, doi:10.1109/WOWMOM.2008.4594857.

[5] S. Sharma, M. Rani, and S. B. Goyal, "Energy efficient data dissemination with ATIM window and dynamic sink in wireless sensor networks," Proc. International Conference on Advances in Recent Technologies in Communication and Computing (ARTCom'09), IEEE Press, Oct. 2009, pp. 559–564, doi:10.1109/ARTCom.2009.9.

[6] S. Tang et al., "DAWN: energy efficient data aggregation in WSN with mobile sinks," Proc. 18th International Workshop on Quality of Service (IWQoS'10), IEEE Press, Jun. 2010, pp. 1–9, doi:10.1109/IWQoS.2010.5542765.

[7] B. Nazir and H. Hasbullah, "Mobile sink based routing protocol (MSRP) for prolonging network lifetime in clustered wireless sensor network," Proc. International Conference on Computer Applications & Industrial Electronics (ICCAIE'10), IEEE Press, Dec. 2010, pp. 624–629, doi:10.1109/ICCAIE.2010.5735010.

[8] K. Mikhaylov and J. Tervonen, "Energy–efficient routing in wireless sensor networks using power–source type identification," Int. J. of Space-Based and Situated Computing, vol. 2, no. 4, Oct. 2012, pp. 253–266, doi:10.1504/IJSSC.2012.050008.

[9] A. A. Somasundara, A. Kansal, D. D. Jea, D. Estrin, and M. B. Srivastava, "Controllably mobile infrastructure for low energy embedded networks," IEEE Trans. Mobile Computing, vol. 5, no. 8, Aug. 2006, pp. 958–973, doi:10.1109/TMC.2006.109.

[10] iRobot Corporation, "iRobot 510 PackBot," url:http://www.irobot.com/en/us/robots/defense/packbot/~/media/Files/Robots/Defense/PackBot/iRobot-510-PackBot-Specs.ashx.

[11] B. Mcbride, R. Longoria, and E. Krotkov, "Measurement and prediction of the off-road mobility of small robotic ground vehicles," Proc. Performance Metrics for Intelligent Systems Workshop (PerMIS'03), Sep. 2003, pp. 1–8.

[12] F. El-Moukaddem, E. Torng, G. Xing, and S. Kulkarni, "Mobile relay configuration in data-intensive wireless sensor networks," Proc. IEEE International Conference on Mobile Adhoc and Sensor Systems (MASS'09), IEEE Press, Oct. 2009, pp. 80–89, doi:10.1109/MOBHOC.2009.5336920.

[13] G. Wang, M. J. Irwin, P. Berman, H. Fu, and T. La Porta, "Optimizing sensor movement planning for energy efficiency," Proc. International Symposium on Low Power Electronics and Design (ISLPED'05), IEEE Press, Aug. 2005, pp. 215–220, doi:10.1109/LPE.2005.195517.

[14] N. Shigei, I. Fukuyama, H. Miyajima, and Y. Yudo, "Battery aware mobile relay for wireless sensor network," Proc. International MultiConference of Engineers and Computer Scientists, IAENG, Mar. 2012, vol. 1, pp. 164–169.

[15] W. Wang, V. Srinivasan, and K.-C. Chua, "Extending the lifetime of wireless sensor networks through mobile relays," IEEE/ACM Transactions on Networking, vol. 16, no. 5, Oct. 2008, pp. 1108 – 1120, doi:10.1109/TNET.2007.906663.

[16] Y. Yun and Y. Xia, "Maximizing the lifetime of wireless sensor networks with mobile sink in delay-tolerant applications," IEEE Transactions on Mobile Computing, vol. 9, no. 9, Sep. 2010, pp. 1308 –1318, doi:10.1109/TMC.2010.76.

[17] C. Chen, J. Ma, and K. Yu, "Designing energy-efficient wireless sensor networks with mobile sinks," Proc. The ACM Conference on Embedded Networked Sensor Systems (Sensys'06), ACM, Oct. 2006, pp. 1–9.

[18] W. Liang and J. Luo, "Network lifetime maximization in sensor networks with multiple mobile sinks," Proc. IEEE Conference on Local Computer Networks (LCN'11), IEEE Press, Oct. 2011, pp. 350–357, doi:10.1109/LCN.2011.6115315.

[19] Texas Instruments, "Stellaris® LM3S9B92 Robotic Evaluation Board," url:http://www.ti.com/lit/ml/spmt213/spmt213.pdf.

[20] K. Mikhaylov, J. Tervonen, and D. Fadeev, "Development of energy efficiency aware applications using commercial low power embedded systems," in Embedded systems - theory and design methodology, K. Tanaka, Ed. Rijeka, Croatia: InTech, 2012, pp. 407–430.

[21] M.-K. Byeon, J.-H. Jeon, and S.-J. Park, "Point-to-multipoint ultrasonic communication modem for ubiquitous underwater wireless sensor networks," Proc. IEEE/IFIP Internation Conference on Embedded and Ubiquitous Computing (EUC'08), IEEE Press, 2008, pp. 685–688, doi:10.1109/EUC.2008.180.

[22] D. Anguita, D. Brizzolara, and G. Parodi, "Building an underwater wireless sensor network based on optical: communication: research challenges and current results," Proc. International Conference on Sensor Technologies and Applications (SENSORCOMM'09), IEEE Press, Sep. 2009, pp. 476–479, doi:10.1109/SENSORCOMM.2009.79.

[23] J. Mathews, M. Barnes, and D. K. Arvind, "Low power free space optical communication in wireless sensor networks," Proc. Euromicro Conference on Digital System Design, Architectures, Methods and Tools (DSD'09), Aug. 2009, pp. 849–856, doi:10.1109/DSD.2009.234.

[24] Texas Instruments, "Stellaris® LM3S9B92 Microcontroller," url:http://www.ti.com/lit/ds/symlink/lm3s9b92.pdf.

[25] Texas Instruments, "A True System-on-Chip solution for 2.4 GHz IEEE 802.15.4 / ZigBee," url:http://www.ti.com/lit/ds/symlink/cc2430.pdf.

[26] Z. Nakutis, "Embedded systems power consumption measurement methods overview," MATAVIMAI, vol. 2, no. 44, 2009, pp. 29–35.

[27] K. Mikhaylov and J. Tervonen, "Optimization of microcontroller hardware parameters for wireless sensor network node power consumption and lifetime improvement," Proc. International Congress on Ultra Modern Telecommunications and Control Systems (ICUMT'10), IEEE Press, Oct. 2010, pp. 1150–1156, doi:10.1109/ICUMT.2010.5676525.

[28] K. Mikhaylov and J. Tervonen, "Evaluation of power efficiency for digital serial interfaces of microcontrollers," Proc. International Conference on New Technologies, Mobility and Security (NTMS'12), IEEE Press, May 2012, pp. 1–5, doi:10.1109/NTMS.2012.6208716.

[29] W. Y. Poe and J. B. Schmitt, "Self-organized sink placement in large-scale wireless sensor networks," Proc. IEEE International Symposium on Modeling, Analysis Simulation of Computer and Telecommunication Systems (MASCOTS'09), IEEE Press, Sep. 2009, pp. 1–3, doi:10.1109/MASCOT.2009.5366741.

[30] F. El-Moukaddem, E. Torng, and G. Xing, "Maximizing network topology lifetime using mobile node rotation," in Wireless Algorithms, Systems, and Applications, vol. 7405, X. Wang, R. Zheng, T. Jing, and K. Xing, Eds. Berlin, Heidelberg: Springer Berlin Heidelberg, 2012, pp. 154–165.